Articles

Evaluation of 3-Carboxy-4(1*H*)-quinolones as Inhibitors of Human Protein Kinase CK2

Andriy G. Golub,[†] Olexander Ya. Yakovenko,[†] Volodymyr G. Bdzhola,[†] Vladislav M. Sapelkin,[†] Piotr Zien,[‡] and Sergiy M. Yarmoluk*,[†]

Institute of Molecular Biology and Genetics of National Academy of Sciences of Ukraine, 150 Zabolotny str., Kyiv 03143, Ukraine, and Adamed Ltd., Department of Oncology, Pienkow 149, 05−152 Czosnow k/W-wy, Warsaw, Poland

Received January 17, 2005

Due to the emerging role of protein kinase CK2 as a molecule that participates not only in the development of some cancers but also in viral infections and inflammatory failures, small organic inhibitors of CK2, besides application in scientific research, may have therapeutic significance. In this paper, we present a new class of CK2 inhibitors—3-carboxy-4(1*H*)-quinolones. This class of inhibitors has been selected via receptor-based virtual screening of the Otava compound library. It was revealed that the most active compounds, 5,6,8-trichloro-4-oxo-1,4-dihydroquinoline-3-carboxylic acid (**7**) (IC_{50} = 0.3 μM) and 4-oxo-1,4-dihydrobenzo[*h*]quinoline-3-carboxylic acid (**9**) (IC_{50} = 1 μM), are ATP competitive (K_i values are 0.06 and 0.28 μM, respectively). Evaluation of the inhibitors on seven protein kinases shows considerable selectivity toward CK2. According to theoretical calculations and experimental data, a structural model describing the key features of 3-carboxy-4(1*H*)-quinolones responsible for tight binding to CK2 active site has been developed.

Introduction

Protein kinase CK2 is involved in the phosphorylation of a large variety of different cellular proteins, among which are the factors of cell growth and transcription, as well as the regulators of cell cycle and apoptosis.[1,2] The CK2 holoenzyme is a heterotetramer consisting of two catalytic subunits (α and α′) and two identical regulatory β-subunits.[3] Interestingly, CK2 demonstrates "dual cosubstrate specificity", using both GTP and ATP as a phosphate donor. Cosubstrate preference depends on the Mg^{2+}—Mn^{2+} ion concentration balance.[4] CK2 can phosphorylate tyrosine in addition to classic serine/threonine residues; thus, this kinase possesses also dual-substrate specificity.[5,6]

Abnormal CK2 expression and function are associated with a number of pathologies, including inflammatory, infectious, and carcinogenic processes. It has been reported that the overexpression of CK2 is associated with cell transformation and neoplasia.[7−10] It has also been revealed that some viruses use CK2 to phosphorylate functionally critical proteins encoded in their genome; consequently, the important role of CK2 in the development of viral infections has been shown.[11] These studies evoke strong interest in this enzyme as a target for anticancer, anti-inflammatory, and anti-infectious drugs.[12]

Nowadays, several classes of CK2 ATP-competitive inhibitors have been reported. These are benzimidazole and benzotriazole derivatives,[13−15] flavonoids,[8,16−18] antraquinones,[19,20] quinazolines,[21,22] quinolines,[23] polypeptide,[24,25] and polysaccharide[26] inhibitors. Among them, potent inhibitors are TBB (4,5,6,7-tetrabromobenzotriazole), DRB (5,6-dichloro-1-β-D-ribofuranosylbenzimidazole), emodin (6-methyl-1,3,8-trihydroxyanthraquinone), and IQA {[5-oxo-5,6-dihydroindolo[1,2-*a*]quinazolin-7-yl]acetic acid}. TBB displays an IC_{50} of about 1.6 μM and high selectivity toward CK2 among a panel of 30 kinases,[13] while DRB (IC_{50} = 6 μM) [15] and emodin (IC_{50} = 0.89 μM) [27] are less specific. The most promising CK2 inhibitor known to date is the IQA (IC_{50} = 0.39 μM),[28,29] which possesses a remarkable selectivity toward CK2 both in vitro and in vivo.

The reported inhibitors act by competing with ATP and partially occupying the CK2 ATP-binding site, forming van der Waals and hydrogen bonds. Since the protein kinase ATP binding site is highly conserved,[30] the design of selective ATP-competitive inhibitors is not an easy task. However, the X-ray analysis of the CK2 structure reveals some important differences in comparison with other kinase family proteins. CK2 appears to have a more compact and hydrophobic ATP/GTP-binding site.[31] There are two unique amino acid residues, Val66 and Ile174,[14] which are replaced in most protein kinases by small and less hydrophobic residues.[16] Mutations in positions 66 and 174 result in the decreased activity of selective inhibitors and loss of CK2 resistance to nonspecific inhibitors.[17] Therefore, CK2 has rather unique determinants for design of highly specific inhibitors.

In the present study we report the evaluation of a new class of CK2 inhibitors—3-carboxy-4(1*H*)-quinolones (Chart 1).

4(1*H*)-Quinolones exhibit a few different biological activities, as immunomodulators,[32] antibacterial compounds that inhibit DNA gyrase (a type II topoisomerase),[33] and antineoplastic compounds that inhibit eukaryotic topoisomerase II.[34] For this class, inhibitory activity toward protein kinases has been reported for 3-phenyl-4(1*H*)-quinolones,[35] which are known EGFR tyrosine kinase inhibitors. The inhibitory activity of this class of compounds toward CK2 has not been investigated previously.

Some 3-carboxy-4(1*H*)-quinolones were revealed to be a CK2 inhibitors after receptor-based virtual screening (docking) of around 70 000 compounds, coming from the Otava compound library. The compounds with high docking scores were selected

* Corresponding author. Phone: (38044) 5222458. Fax: (38044) 5222458. E-mail: sergiy@yarmoluk.org.ua.
[†] Institute of Molecular Biology and Genetics of National Academy of Sciences of Ukraine.
[‡] Adamed Ltd.

10.1021/jm050048t CCC: $33.50
Published on Web 09/29/2006

Chart 1. Structure of the 3-Carboxy-4(1*H*)-quinolones

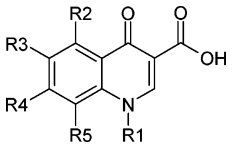

for in vitro tests. Nine 3-carboxy-4(1*H*)-quinolones were tested, and 5,6,8-trichloro-4-oxo-1,4-dihydroquinoline-3-carboxylic acid (**7**) and 4-oxo-1,4-dihydrobenzo[*h*]quinoline-3-carboxylic acid (**9**) displayed IC_{50} values of 0.3 and 1 μM, respectively. The presence of CK2 inhibitors among 3-carboxy-4(1*H*)-quinolones encouraged us to investigate other derivatives of this class in order to determine the effect of certain substituents on their inhibitory activity. The binding mode of 3-carboxy-4(1*H*)-quinolones in the CK2 ATP binding site, obtained through docking and molecular dynamics simulation experiments, is discussed. Additionally, a comparative study with the IQA−CK2 complex was performed.

Results and Discussion

(a) Virtual Screening. To screen the set of 70 000 compounds we used the docking technique as a part of our DOCK-based screening system. The best-scored set of compounds, containing nine 3-carboxy-4(1*H*)-quinolones (**1**−**9**, see Table 1), was proceeded to in vitro tests.

(b) In Vitro Tests. Two compounds (**7** and **9**) from nine 3-carboxy-4(1*H*)-quinolones that were selected by the DOCK showed remarkable CK2 inhibitory activity in vitro (Table 1). It was contribution for further studies of 3-carboxy-4(1*H*) quinolone (Table 1) and 3-carbethoxy-4(1*H*)-quinolone derivatives. Data for the carbethoxy derivatives are not presented because the most active ones revealed an IC_{50} of about 40 μM.

Two 3-carboxy-4(1*H*)-quinolones, **7** and **9**, were selected for further studies. IC_{50} values for these active compounds are 0.3 and 1 μM, respectively (Table 1). To investigate the mechanism of action of the obtained inhibitors, kinetic experiments were performed with different concentrations of both ATP and

Table 1. Structure of 3-Carboxy-4(1*H*)-quinolone Derivatives and Their Activity toward CK2

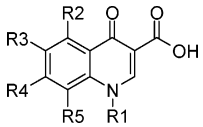

compd	R1	R2	R3	R4	R5	CK2 activity,[a] %	IC_{50} values,[b] μM
1	H	H	I	H	H	85	
2	H	H	CO_2H	H	H	91	
3	H	H	H	CO_2H	H	74	
4	H	H	H	H	CO_2H	73	
5	H	H		$-OCH_2CH_2O-$	H	81	
6	H	H	Cl	H	Cl	64	
7	H	Cl	Cl	H	Cl	2.6	0.3
8	H	H	F	F	OCH_2-	88	
9	H	H	H	$-CH=CH=CH=CH-$		4.5	1
10	H	H	OEt	H	H	107	
11	H	H	OMe	H	H	101	
12	H	H	H	H	H	103	
13	H	H	H	H	OEt	103	
14	H	H	F	*N*-methylpiperazino	$OCH_2CH(CH_3)N_1$	100	
15	H	H	Me	H	H	100	
16	H	H	$COCH_3$	H	H	100	
17	H	H	OMe	H	Ome	99	
18	H	H	H	H	i-Pr	95	
19	H	H	OPr-i	H	H	93	
20	H	H	H	H	OMe	92	
21	H	H	OC_6H_5	H	H	89	
22	H	H	C_4H_9	H	H	87	
23	H	H	H	H	Et	86	
24	H	H	OPr	H	H	80	
25	H	H	H	CF_3	H	78	
26	H	H	Br	H	H	76	
27	H	H	Cl	H	H	75	
28	H	H	NMe_2	H	H	75	
29	H	H	H	H	Me	74	
30	H	H	F	H	H	72	
31	H	H	H	H	F	70	
32	H	Cl	H	Cl	H	70	
33	H	H	Me	H	Me	63	
34	H	H	H	Me	Me	56	
35	H	H	H	H	Br	42	
36	H	H	H	H	Cl	37	
37	H	Me	H	H	Me	32	
38	H	H	H	Cl	Me	15	2
39	H	H	H	Cl	Cl	12.5	0.8
40	Me	H	H	H	H	106	
41	Me	H	Me	H	Me	102	
42	Me	H	Me	H	H	100	

[a] At 30 μM of compound. [b] IC_{50} values are indicated for compounds inhibiting the CK2 activity more than 80%.

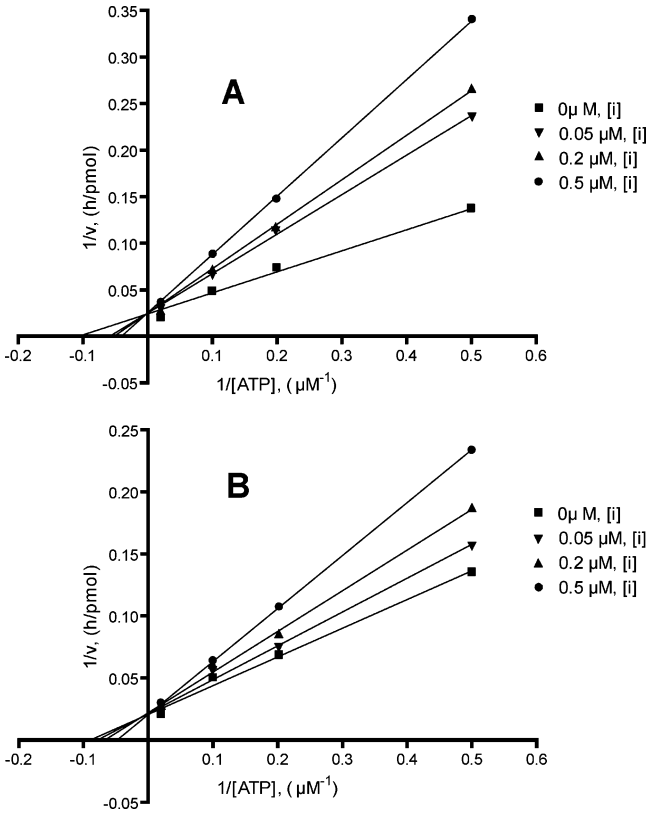

Figure 1. Lineweaver−Burk plots of CK2 inhibition by compounds **7** (A) and **9** (B). K_i values are 0.06 and 0.28 μM, respectively. Concentration of inhibitors varied from 0 to 0.5 μM. Enzyme activities were assayed as described in Experimental Section.

inhibitors. These experiments demonstrate that inhibitors **7** and **9** are ATP competitive, revealing K_i values of 0.06 and 0.28 μM, respectively (Figure 1).

The selectivity of the inhibitors **7** and **9** was tested in vitro on five serine/threonine and two tyrosine kinases (Table 2). As can be observed from the table, the inhibitors show considerable specificity toward CK2. The exception is DYRK1, which revealed residual activity of 35% for inhibitor **7**. It should be noted that the most specific CK2 inhibitors known to date (TBB and IQA) also affect DYRK1 more strongly than 31 other investigated kinases, showing an IC_{50} of 1 and 8 μM, respectively.[29]

Table 2. Specificity Spectrum of Inhibitors **7** and **9**[a]

protein kinase	inhibitor **7**	inhibitor **9**	protein kinase	inhibitor **7**	inhibitor **9**
CK2	11	25	DYRK1a	35	85
JNK3	74	81	MSK1	71	89
ROCK-I	85	78	GSK3	>50	>50
p56 LCK	87	80	CDK5	>50	>50

[a] Residual activity determined in the presence of 10 μM inhibitor is expressed as a percentage of the control without inhibitor. Final concentration of ATP in the experiment was 100 μM.

(c) Molecular Dynamics: Analysis of the Binding Mode. It is difficult to explain the molecular mechanism of inhibitor binding to CK2 on the basis of the docking data alone, because the protein molecule remains rigid during the virtual screening. To investigate the binding features of the discovered inhibitors, we performed 2-ns molecular dynamics (MD) simulation of the CK2 complexes with inhibitors **7** and **9**.

Initially, several different simulations were launched, using four different inhibitor start positions in the active site and the ionized/nonionized state of the ligand carboxy group (p*K* value for 3-carboxy-4(1*H*)-quinolones is ~6.51).[44] For each ligand, the only "survived" launch was (a) the nonionized state and (b) the starting position obtained with docking. All other variants resulted in protein−ligand complex dissociation at about 0.5 ns of the simulation and release of the ligand from the active site into the water environment. The dissociation can be explained by (i) an incorrect starting position of the ligand and/or (ii) the presence of a negative charge on the ionized carboxy group, which causes electrostatic repulsion with negatively charged Asp174 and Glu81.

The results of MD simulation allowed us to make the following deductions. Generally, the investigated inhibitors **7** and **9** are characterized by similar binding mode. They occupy the CK2 ATP-binding site, where they interact with the hydrophobic pocket formed by residues of the hinge region and adjacent residues of C-terminal and N-terminal lobes and form hydrogen bonds with Lys68 and Asp175. These interactions in both cases are present all the time during MD simulation. The hydrogen

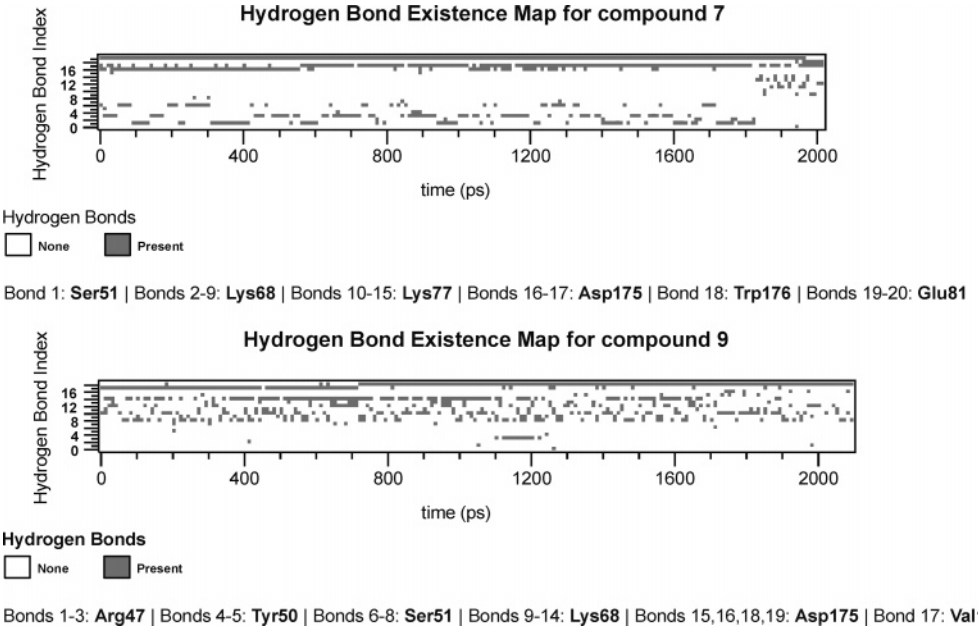

Figure 2. Hydrogen-bond existence maps of **7**−CK2 and **9**−CK2 complexes during 2-ns MD simulation.

Table 3. Hydrogen Bonds Formed by Inhibitor 7 with Amino Acid Residues of CK2 Active Site during 2-ns Molecular Dynamics Simulation

no.	donor	hydrogen	acceptor
1	SER51 OG	SER51 HG	**7** O
2	LYS68 NZ	LYS68 HZ1	**7** O
3	LYS68 NZ	LYS68 HZ1	**7** O10
4	LYS68 NZ	LYS68 HZ2	**7** O
5	LYS68 NZ	LYS68 HZ2	**7** O10
6	LYS68 NZ	LYS68 HZ2	**7** O00
7	LYS68 NZ	LYS68 HZ3	**7** O
8	LYS68 NZ	LYS68 HZ3	**7** O10
9	LYS68 NZ	LYS68 HZ3	**7** O00
10	LYS77 NZ	LYS77 HZ1	**7** O10
11	LYS77 NZ	LYS77 HZ1	**7** O00
12	LYS77 NZ	LYS77 HZ2	**7** O10
13	LYS77 NZ	LYS77 HZ2	**7** O00
14	LYS77 NZ	LYS77 HZ3	**7** O10
15	LYS77 NZ	LYS77 HZ3	**7** O00
16	ASP175 N	ASP175 H	**7** O
17	ASP175 N	ASP175 H	**7** O10
18	TRP176 N	TRP176 H	**7** O10
19	**7** O00	**7** HO	GLU81 OE1
20	**7** O00	**7** HO	GLU81 OE2

Table 4. Hydrogen Bonds Formed by Inhibitor **9** with Amino Acid Residues of CK2 Active Site during 2-ns Molecular Dynamics Simulation

no.	donor	hydrogen	acceptor
1	ARG 47 N	ARG 47 H	**9** O
2	ARG 47 NH1	ARG 47 HH11	**9** O
3	ARG 47 NH2	ARG 47 HH21	**9** O
4	TYR 50 OH	TYR 50 HH	**9** O
5	TYR 50 OH	TYR 50 HH	**9** O10
6	SER 51 OG	SER 51 HG	**9** O
7	SER 51 OG	SER 51 HG	**9** O10
8	SER 51 OG	SER 51 HG	**9** O00
9	LYS 68 NZ	LYS 68 HZ1	**9** O10
10	LYS 68 NZ	LYS 68 HZ1	**9** O00
11	LYS 68 NZ	LYS 68 HZ2	**9** O10
12	LYS 68 NZ	LYS 68 HZ2	**9** O00
13	LYS 68 NZ	LYS 68 HZ3	**9** O10
14	LYS 68 NZ	LYS 68 HZ3	**9** O00
15	ASP 175 N	ASP 175 H	**9** O10
16	ASP 175 N	ASP 175 H	**9** O00
17	**9** N	**9** HN	VAL 116 O
18	**9** O00	**9** HO	ASP 175 OD1
19	**9** O00	**9** HO	ASP 175 OD2

bond (HB) existence maps for inhibitors **7** and **9** calculated by GROMACS are represented in Figure 2. HB maps show long-term hydrogen bonds formed, on one hand, by oxygens of the carboxy group of ligands and, on the other hand, by the backbone nitrogen of Asp175 and the side chain nitrogen of Lys68 (Tables 3 and 4). There is an additional long-term hydrogen bond formed between the inhibitor **7** nonionized carboxy group and the ionized carboxylic acid group of the Glu81 side chain.

During dynamics, three residues (Asp175, Lys68, and Glu81) are connected by hydrogen bonds to each other, and these contacts are critical for the support of the active site spatial structure. Inspection of CK2 crystal structures available by that time in the Brookhaven Protein Data Bank shows that hydrogen bonds between Lys68, Asp175, and Glu81 are present in all of them. MD studies show that compounds **7** and **9** bind to these residues through insertion of a carboxy group, which results in partial rearrangement of the aforementioned hydrogen bonds.

Also, the short-term hydrogen bonds are formed during dynamics both for inhibitors **7** and **9** (see Figure 2). These hydrogen bonds are unstable but are the essential feature of the dynamic protein−ligand system. Among them the H-bonds between the side chains of Ser51 and Lys68 and the oxygen in

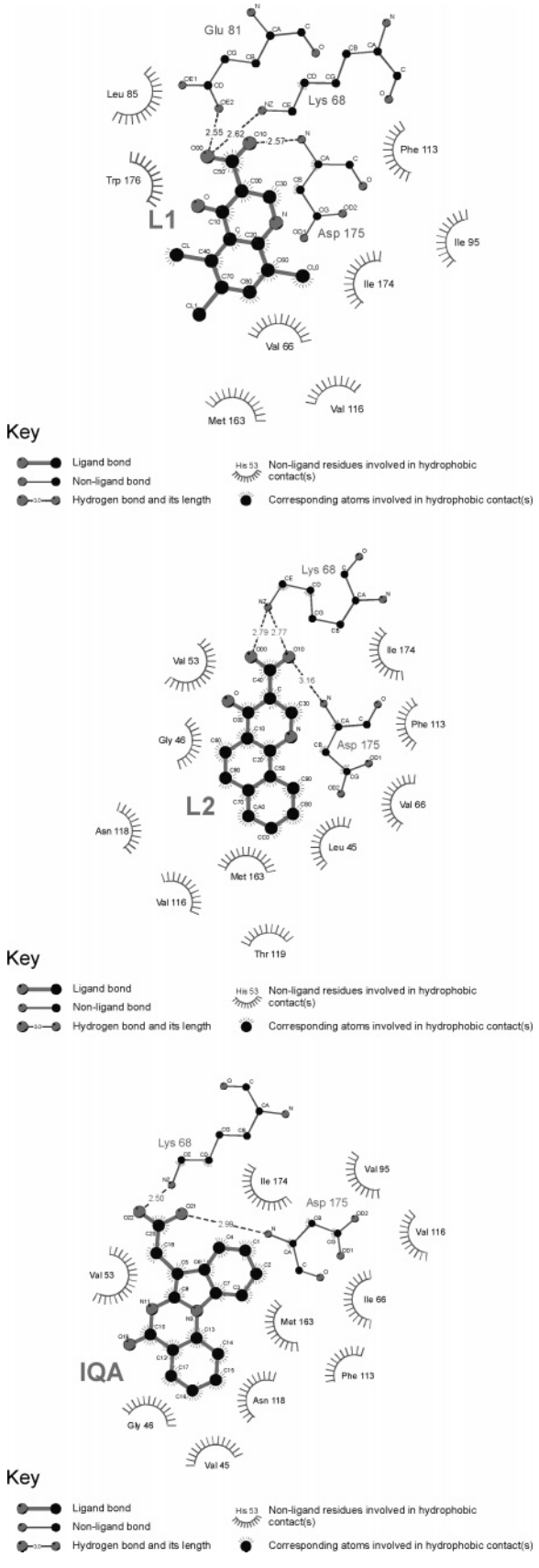

Figure 3. Interaction plots for **7**−CK2 and **9**−CK2 complexes (molecular dynamics snapshots). For comparison, the interaction plot for IQA (crystal structure of CK2−IQA complex) is also showed. The plots were produced with LigPlot software.[47] For detailed information on the atom−atom contacts, please refer to the Tables 5−7 of the Supporting Information.

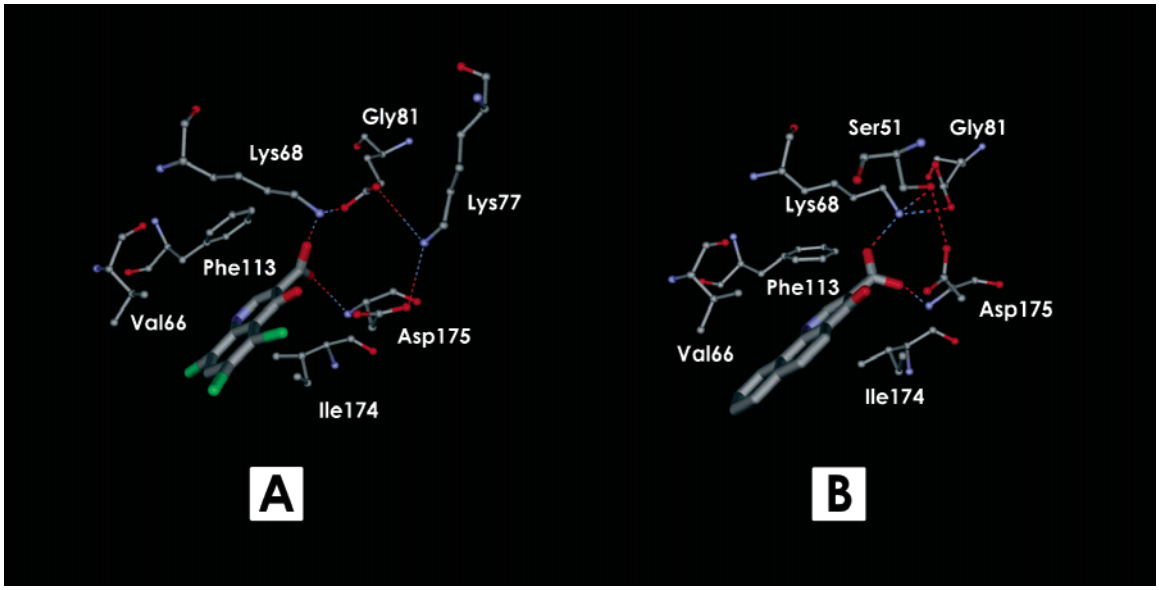

Figure 4. 3D representation of the structural model that characterizes binding features of the inhibitors **7** (A) and **9** (B). The most important intermolecular and intramolecular hydrogen bonds are represented as dashed lines. The CK2 amino acid residues involved in key hydrophobic interactions with the ligand are indicated as well. For detailed information on the atom−atom contacts, please refer to the Tables 5 and 6 of the Supporting Information.

the fourth position of the ligands should be mentioned as an additional factor that contributes to the stability of the complex.

The residues Trp176, Asp175, Ile174, Met163, Val116, Phe113, Ile95, Leu85, Glu81, Lys68, and Val66 of the CK2 ATP-binding site are involved in hydrophobic contacts with inhibitor **7** (see Figure 3 and Table 5 of the Supporting Information). The major contributions to the hydrophobic interactions are provided by Phe113, Val66, and Ile174. These residues take part in the clamping of the inhibitor **7** heterocyclic ring and, therefore, in stabilization of the ligand in the active site.

Inhibitor **9** hydrophobic contacts are represented by residues Asp175, Ile174, Met163, Thr119, Asn118, Val116, Phe113, Lys68, Val66, Val53, Gly46, and Leu45. Here we indicate weak hydrophobic interactions with Phe113, but strong contacts with Ile174 and Val66 are preserved (see Figure 3 and Table 6 of the Supporting Information).

The molecular dynamics snapshots characterizing the binding mode of inhibitors **7** and **9** are represented in Figures3 and 4. The binding features developed for inhibitors **7** and **9** appear to be similar to ones for IQA, a known CK2 inhibitor.[29] The IQA carboxy group occupies the same position in the CK2 ATP binding site and forms the hydrogen bonds with residues Lys68 and Asp175. IQA is also characterized by the similar hydrophobic interactions with CK2 (see Figure 3 and Tables 5−7 of the Supporting Information).

(d) Structure−Activity Relationships. On the basis of in vitro activity data on 4(1*H*)-quinolone derivatives and according to the proposed model of CK2-inhibitor interactions, we are able to observe the effect of certain substituents on the inhibitor biological activity.

The key substituent is the 3-carboxy group. It makes essential contribution to the affinity of 4(1*H*)-quinolone derivatives. In contrast to 3-carboxy derivatives, 3-carbethoxy derivatives were shown to have low activity toward CK2. According to the proposed binding model, this fact could be explained by formation of stable hydrogen bonds between the 3-carboxy group and ATP-binding site residues Lys68 and Asp175. The results of MD simulation reveal that these H-bonds remain stable upon rotation of the carboxy group, while the carbethoxy group in turn seems to be less favorable for H-bond formation due to steric hindrances and, in consequence, results in destabilization of the ligand in the CK2 active site. For example, the etheric derivatives of compounds **7** and **9** revealed high IC_{50} values (about 40 μM).

The R4 and R5 substituents of the scaffold are of special interest. The presence of hydrophobic atoms in R4 and R5 positively affects the inhibitory activity. This effect depends on the hydrophobicity of the substituent, and replacement of the chlorine atom in R5 and R4 by less hydrophobic CH_3[36] decreases the activity (**39** ($IC_{50} = 0.8$ μM), **38** ($IC_{50} = 2$ μM), and **34** ($IC_{50} \geq 33$ μM)). The favorable effect of hydrophobic substitution in this position can be explained by its contacts with hydrophobic residues Val66 and Ile174, which are the unique feature of the CK2 ATP-binding site. It should also be noted that the presence of hydrophobic but relatively bulky groups in R5, such as ethyl or isopropyl, has negative effect on activity. Described influences of the substituents R4 and R5 on the inhibitory activity were also observed for 3-carbethoxy derivatives (data not shown). Therefore, optimization of the scaffold at this position is the most advantageous but possibly limited due to steric hindrances at the region formed by bulky residues Val66 and Ile174.

Substituents R2 and R3 are less important for the inhibitory activity. Variations in these positions result in insignificant changes in activity, possibly because of weak interactions with CK2 active site residues.

Conclusions

Using a virtual screening technique we have identified 3-carboxy-4(1*H*)-quinolones as a new class of ATP-competitive CK2 inhibitors. Docking and molecular dynamics studies allowed us to propose a binding mode in which the key interactions are hydrogen bonds between the ligand's 3-carboxy group and two residues (Lys68 and Asp175) of the CK2 ATP-binding cleft, as well as hydrophobic contacts with Val66, Ile174, and Phe113. The obtained model correlates well with X-ray data for the complex CK2−IQA. Selectivity tests have

Scheme 1. Synthesis of Compounds **1**−**42**[a]

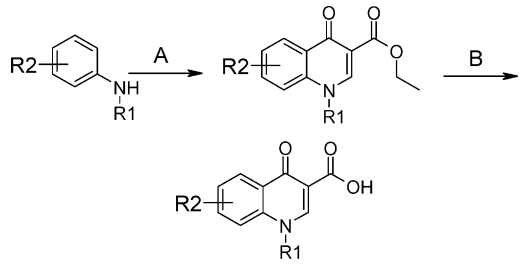

[a] Reagents and conditions: (A) diethyl ethoxymethylenemalonate, 220−230 °C; (B) (1) NaOH, H_2O, refluxing; (2) HCl.

shown considerable selectivity of the inhibitors **7** and **9** toward CK2. The identified inhibitors may be of interest for further structural optimization and biological evaluation.

Experimental Section

(a) Software Background. Receptor molecule was prepared with the GROMACS[37] molecular dynamic package, Connoly MS,[38] and Grid from DOCK 4.0.[39−42] Ligand molecules were processed with GAMESS,[43] GROMACS, and TOPBUILDER in-house software. Molecular docking was performed by DOCK within DOCK 4.0.

(b) Receptor Preparation. The crystal structure of human CK2 holoenzyme was obtained from the Brookhaven Protein Data Bank (PDB ID: 1jwh).[9] The catalytic α subunit has been extracted from the pdb file, and the ATP molecule has been removed from the CK2−ATP complex.

The receptor molecule has been minimized in water with the GROMACS molecular dynamics simulation package (GROMACS force field, steepest descent algorithm, 1000 steps, em_tolerance = 100, em_step = 0.001). The partial atom charges of the receptor molecule were taken from the Amber force field. Active site spheres were calculated with the DOCK *sphgen* software. Thirty-one spheres from the largest cluster of 37 spheres were selected to fill the receptor active site, and six spheres were deleted manually since their positions were localized outside of the active site cavity. The Connoly MS and Grid programs from DOCK package were used to generate the receptor Connoly surface and energy grids.

(c) Ligand Preparation. Ligand molecules have been processed with SCREENER in-house software (preprocessing of input ligand database file, converting 2D structures to 3D), the GROMACS package (fast energy minimization of the ligands by GROMACS force field), and the GAMESS package (complete energy minimization by AM1 semiempirical method, calculation of partial charges). The program TOPBUILDER was used to generate GROMACS-formatted molecular topologies, to control ligand energy minimization in GROMACS and to assign atom partial charges calculated in GAMESS.

(d) Molecular Docking. Flexible molecular docking of the target compound library was performed in the CK2 ATP-binding site by DOCK. The resulted range of docking scores was from −14 to −51 kcal/mol. Compounds with scores below −42 kcal/mol have been chosen as promising ones.

(e) Molecular Dynamics. Molecular dynamics simulation of each CK2−ligand complex was performed with the GROMACS 3.1.2 package (GROMACS force field). The conditions of the MD simulation considered the water solvent and the temperature at 300 K. According to the GROMACS force field, only polar hydrogens of protein molecule were taken into account, and carboxy groups of acidic amino acids were ionized in the simulation.

(f) Chemical Synthesis. Quinolin-4-one 3-carboxylic acids were prepared by general procedure, described for synthesis of 7-chloro-quinolin-4-one 3-carboxylic acid [45] (Scheme 1).

Ethyl α-Carbethoxy-*β*-*m*-chloroanilinoacrylate. A few boiling chips were added to a mixture of 127.5 g (1.0 mol) of *m*-chloroaniline and 233 g (1.1 mol) of ethyl ethoxymethylenemalonate in an open 500-mL round-bottomed flask. The mixture was heated on a steam bath for 1 h, the evolved ethanol being allowed to escape. The warm product was used directly in the next step.

7-Chloro-4-hydroxy-3-quinolinecarboxylic Acid. In a 5-L round-bottomed flask equipped with an air condenser 1 L of Dowtherm A was heated to vigorous boiling, and the product of the above step was poured in through the condenser. Heating was continuing for 1 h, during which time a large proportion of the cyclization product crystallized. The mixture was cooled, filtered, and washed with two 400-mL portions of Skellysolve B (bp 61−70 °C) to remove the major portion of colored impurities. The air-dried filter cake was mixed with 1 L of 10% aqueous sodium hydroxide, and the mixture was refluxed vigorously until all the solid ester dissolves (about 1 h). The saponification mixture was cooled, and the aqueous solution was separated from any oil that may be present. The solution was acidified to Congo red paper with 10% sulfuric acid. The 7-chloro-4-hydroxy-3-quinoline-carboxylic acid (190−220 g, 85−98%) was collected by filtration and washed thoroughly with water. The dry acid melts at about 266 °C with effervescence.

^{1}H NMR spectra were recorded on a Varian VXR-300 spectrometer (300 MHz), and chemical shifts (ppm) were reported relative to tetramethylsilane. Signals were designated as follows: brs, broad singlet; s, singlet; d, doublet; dd, doublet of doublets; t, triplet; q, quartet; m, multiplet. Elemental microanalyses are indicated by symbols of elements, and results were within ±0.4% of the theoretical values.

(g) Biological Testing. Selected compounds were tested using in vitro kinase assay. Each test was performed twice in a total reaction volume of 30 μL, containing 1 μg of peptide substrate RRREEETEEE (New England Biolabs); 10 units of recombinant protein kinase CK2 (New England Biolabs); 50 μM ATP and γ-labeled ATP, diluted to specific activity 100 μCi/μM; CK2 buffer (20 mM Tris-HCl, pH 7.5; 50 mM KCl; 10 mM $MgCl_2$); and inhibitor in varying concentrations. Incubation time was 20 min at 30 °C. The reaction was stopped by adding an equal volume of 10% *o*-phosphoric acid and the reaction mixture was loaded onto a 20 mm disk of phosphocellulose paper (Whatman). Disks were washed three times with 1% *o*-phosphoric acid solution, air-dried at room temperature, and counted by the Cherenkov's method in the β-counter (LKB). An equal volume of DMSO was added as negative control to the reaction mixture instead of inhibitor stock solution. Quercetine, a known CK2 inhibitor,[16] was used as inhibition positive control. The final concentration of quercetine was 0.55 μM (that inhibited the CK2 activity by 50%). Percent of inhibition was calculated from substrate-incorporated radioactivity in testing reaction relative to the radioactivity incorporated in control reactions, i.e., in the absence of any inhibitor. Serial dilutions of inhibitor stock solution were used in reactions to determine their IC_{50} concentrations.

CDK5 and GSK-3 were prepared and assayed as described previously.[46] Protein kinases JNK3, ROCK-I, p56 LCK, DYRK1a, and MSK1 were assayed according to supplier suggestions (Upstate).

Acknowledgment. This investigation was supported by grant from the National Academy of Sciences of Ukraine. We thank Dr. Laurent Meijer and Dr. Olivier Lozach (Laboratory of Molecular & Cellular Neuroscience, The Rockefeller University) for performing the CDK and GSK-3 assays and for helpful comments on the manuscript.

Supporting Information Available: Tables of atom−atom contacts, spectroscopic data, and elemental analysis results. This material is available free of charge via the Internet at http://pubs.acs.org.

References

(1) Allende, J. E.; Allende, C. C. Protein Kinase CK2: An Enzyme with Multiple Substrates and a Puzzling Regulation. *FASEB J.* **1995**, *9*, 313−323.

(2) Pinna, L. Protein Kinase CK2. *Int. J. Biochem. Cell. Biol.* **1997**, *29*, 551−554.
(3) Niefind, K.; Guerra, B.; Ermakowa, I.; Issinger, O. G. Crystal Structure of Human Protein Kinase CK2: Insights into Basic Properties of the CK2 Holoenzyme. *EMBO J.* **2001**, *20*, 19, 5320−5331.
(4) Tuazon, P. T.; Traugh, J. A. Casein kinase I and II. Multipotential Serine Protein Kinases: Structure, Function and Regulation. In *Advances in Second Messenger and Phosphoprotein Research;* Greengard, P., Robison, G. A., Eds; Raven Press: Ltd.: New York, 1991; Vol. 23, pp 123−164.
(5) Lindberg, R. A.; Quinn, A. M.; Hunter, T. Dual-Specificity Protein Kinases: Will Any Hydroxyl Do? *Trends Biochem. Sci* **1992**, *17*, 114−119.
(6) Wilson, L. K.; Dhillon, N.; Thorner, J.; Martin, G. S. Casein Kinase II Catalyzes Tyrosine Phosphorylation of the Yeast Nucleolar Immunophilin Fpr3. *J. Biol. Chem.* **1997**, *272*, 12961−12967.
(7) Unger, G. M.; Davis, A. T.; Slaton, J. W.; Ahmed, K. Protein Kinase CK2 as Regulator of Cell Survival: Implications for Cancer Therapy. *Curr. Cancer Drug Targets* **2004**, *4*, 77−84.
(8) Kelliher, M. A.; Seldin, D. C.; Leder, P. Tal-1 Induces T Cell Acute Lymphoblastic Leukemia Accelerated by Casein Kinase Iialpha. *EMBO J.* **1996**, *15*, 5160−5166.
(9) Orlandini, M.; Semplici, F.; Ferruzzi, R.; Meggio, F.; Pinna, L. A.; Oliviero, S. Protein Kinase CK2alpha′ Is Induced by Serum as a Delayed Early Gene and Cooperates with Ha-ras in Fibroblast Transformation. *J. Biol. Chem.* **1998**, *273*, 21291−21297.
(10) Landesman-Bollag, E.; Channavajhala, P. L.; Cardiff, R. D.; Seldin, D. C. p35 Deficiency and Misexpression of Protein Kinase CK2a Collaborate in the Development of Thymic Lymphomas in Mice. *Oncogene* **1998**, *23*, 2965−2974.
(11) Pinna, L. A.; Meggio, F. Protein Kinase CK2 ("casein kinase-2") and Its Implication in Cell Division and Proliferation. *Prog. Cell Cycle Res.* **1997**, *3*, 77−97.
(12) Ravi, R.; Bedi, A. Sensitization of Tumor Cells to Apo2 Ligand/TRAIL-Induced Apoptosis by Inhibition of Casein Kinase II. *Cancer Res.* **2002**, *62*, 4180−4185.
(13) Sarno, S.; Reddy, H.; Meggio, F.; Ruzzene, M.; Davies, S. P.; Donella-Deana, A.; Shugar, D.; Pinna, L. Selectivity of 4,5,6,7-Tetrabromobenzotriazole, an ATP Site-Directed Inhibitor of Protein Kinase CK2 ("casein kinase"). *FEBS Lett.* **2001**, *496*, 44−48.
(14) Battistutta, R.; De Moliner, E.; Sarno, S.; Zanotti, G.; Pinna, L. A. Structural Features Underlying Selective Inhibition of Protein Kinase CK2 by ATP-Site Directed Tetrabromo-benzotriazole. *Protein Sci.* **2001**, *10*, 2200−2206.
(15) Szyszka, R.; Grankowski, N.; Felczak, K.; Shugar, D. Halogenated Benzimidazoles and Benzotriazoles as Selective Inhibitors of Protein Kinases CK I and CK II from *Saccharomyces cerevisiae* and Other Sources. *Biochem. Bioophys. Res. Commun.* **1995**, *208*, 418−424.
(16) Sarno, S.; Moro, S.; Meggio, F.; Zagotto, G.; Dal Ben, D.; Ghisellini, P.; Battistuta, R.; Zanotti, G.; Pinna, L. Toward the Rational Design of Protein Kinase Casein Kinase-2 Inhibitors. *Pharmacol. Ther.* **2002**, *93*, 159−168.
(17) Davies, S. P.; Reddy, H.; Caivano, M.; Cohen, P. Specificity and Mechanism of Action of Some Commonly Used Protein Kinase Inhibitors. *Biochem. J.* **2000**, *351*, 95−10.
(18) Prykhod'ko, A. O.; Yakovenko, O. Ya.; Golub, A. G.; Bdzhola, V. G.; Yarmoluk, S. M. Evaluation of 4*H*-4-Chromenone Derivatives as Inhibitors of Protein Kinase CK2. *Biopolym. Cell* **2005**, *21*, 2, 1−6.
(19) Yim, H.; Lee, Yh.; Lee, S. K. Emodin, an Anthraquinone Derivative Isolated from the Rhizomes of *Rheum palmatum* Selectively Inhibits the Activity of Casein Kinase II as Competitive Inhibitor. *Planta Med.* **1999**, *65*, 1, 9−13.
(20) Meggio, F.; Pagano, M. A.; Moro, S.; Zagotto, G.; Ruzzene, M.; Sarno, S.; Cozza, G.; Bain, J.; Elliott, M.; Deana, A. D.; Brunati, A. M.; Pinna, L. A. Inhibition of Protein Kinase CK2 by Condensed Polyphenolic Derivatives. An in Vitro and in Vivo Study. *Biochemistry* **2004**, *43*, 12931−12936.
(21) Liu, X. G.; Liang, N. C. Inhibitory Effect and Its Kinetic Analysis of Tyrphostin AG1478 on Recombinant Human Protein Kinase CK2 Holoenzyme. *Acta Pharmacol. Sin.* **2002**, *23*, 6, 556−561.
(22) Sapelkin, V. M.; Golub, A. G.; Yakovenko, O. Ya.; Bdzhola, V. G.; Yarmoluk, S. M. Search for Protein Kinase CK2 Inhibitors among 4-Aminoquinazoline Derivatives. *Ukr. Bioorg. Acta* **2004**, *1*, 74−79.
(23) Sapelkin, V. M.; Golub, A. G.; Yakovenko, O. Ya.; Bdzhola, V. G.; Yarmoluk, S. M. Search for Protein Kinase CK2 Inhibitors among 3-Carboxy-4-aminoquinoline Derivatives. *Ukr. Bioorg. Acta* **2005**, *2*, 28−32.
(24) Meggio, F.; Pinna, L. A.; Marchiori, F.; Borin, G. Polyglutamyl Peptides: A New Class of Inhibitors of Type-2 Casein Kinases. *FEBS Lett.* **1983**, *162*, 235−238.
(25) Tellez, R.; Gatica, M.; Allende, C. C.; Allende, J. E. Copolymers of Glutamic Acid and Tyrosine Are Potent Inhibitors of Oocyte Casein Kinase II. *FEBS Lett.* **1990**, *265*, 113−116.
(26) Hathaway, G. M.; Lubben, T. H.; Traugh, J. A. Inhibition of Casein Kinase II by Heparin. *J. Biol. Chem.* **1980**, *255*, 8038−8041.
(27) Battistutta, R.; Sarno, S.; De Moliner, E.; Papinutto, E.; Zanotti, G.; Pinna, L. A. The Replacement of ATP by the Competitive Inhibitor Emodin Induces Conformational Modifications in the Catalytic Site of Protein Kinase CK2. *J. Biol. Chem.* **2000**, *275*, 29618−29622.
(28) Vangrevelinghe, E.; Zimmermann, K.; Schoepfer, J.; Portmann, R.; Fabbro, D.; Furet, P. Discovery of a Potent and Selective Protein Kinase CK2 Inhibitor by High-Throughput Docking. *J. Med. Chem.* **2003**, *46*, 2656−2662.
(29) Sarno, S.; De Moliner, E.; Ruzzene, M.; Pagano, M. A.; Battistutta, R.; Bain, J.; Fabbro, D.; Schoepfer, J.; Elliott, M.; Furet, P.; Meggio, F.; Zanotti, G.; Pinna, L. A. Biochemical and Three-Dimensional-Structural Study of the Specific Inhibition of Protein Kinase CK2 by [5-Oxo-5,6-dihydroindolo-(1,2-*a*)quinazolin-7-yl]acetic acid (IQA). *Biochem. J.* **2003**, *374*, 639−646.
(30) Manning, G.; Whyte, D. B.; Martinez, R.; Hunter, T.; Sudarsanan, S. The Protein Kinase Complement of the Human Genome. *Science* **2002**, *298*, 1912−1934.
(31) Niefind, K.; Putter, M.; Guerra, B.; Issinger, O. G.; Schomburg, D. GTP Plus Water Mimic ATP in the Active Site of Protein Linase CK2. *Nat. Struct. Biol.* **1999**, *6*, 1100−1103.
(32) Dalhoff, A.; Shalit, I. Immunomodulatory Effects of Quinolones. *Lancet Infect. Dis.* **2003**, *3*, 359−371.
(33) Drlica, K.; Zhao, X. DNA Gyrase, Topoisomerase IV, and the 4-Quinolones. *Microbiol. Mol. Biol. Rev.* **1997**, *61*, 377−392.
(34) Robinson, M. J.; Martin, B. A.; Gootz, T. D.; McGuirk, P. R.; Moynihan, M.; Sutcliffe, J. A.; Osheroff, N. Effects of Quinolone Derivatives on Eukaryotic Topoisomerase II. A Novel Mechanism for Enhancement of Enzyme-Mediated DNA Cleavage. *J. Biol. Chem.* **1991**, *266*, 14585−14592.
(35) Traxler, P.; Green, J.; Mett, H.; Séquin, U.; Furet, P. Use of a Pharmacophore Model for the Design of EGFR Tyrosine Kinase Inhibitors: Isoflavones and 3-Phenyl-4(1*H*)-quinolones. *J. Med. Chem.* **1999**, *42*, 1018−1026.
(36) Wang, R.; Fu, Y.; Lai, L. A New Atom-Additive Method for Calculating Partition Coefficients. *J. Chem. Inf. Comput. Sci.* **1997**, *37*, 615−621.
(37) Lindahl, E.; Hess, B.; van der Spoel, D. GROMACS 3.0: A Package for Molecular Simulation and Trajectory Analysis. *J. Mol. Mod.* **2001**, *7*, 306−317.
(38) Connolly, M. L. MS: Molecular Surface Program. 1983, QCPE Program 429, Quantum Chemistry Program Exchange, University of Indiana, Bloomington, IN http://www.netsci.org/Science/Compchem/feature14.html.
(39) Shoichet, B. K.; Stroud, R. M.; Santi, D. V.; Kuntz, I. D.; Perry, K. M. Structure-Based Discovery of Inhibitors of Thymidylate Synthase. *Science* **1993**, *259*, 1445−1450.
(40) Bodian, D. L.; Yamasaki, R. B.; Buswell, R. L.; Stearns, J. F.; White, J. M.; Kuntz, I. D. Inhibition of the Fusion-Inducing Conformational Change of Influenza Hemagglutinin by Benzoquinones and Hydroquinones. *Biochemistry* **1993**, *32*, 2967−2978.
(41) Ring, C. S.; Sun, E.; McKerrow, J. H.; Lee, G. K.; Rosenthal, P. J.; Kuntz, I. D.; Cohen, F. E. Structure-Based Inhibitor Design by Using Protein Models for the Development of Antiparasitic Agents. *Proc. Natl. Acad. Sci. U.S.A.* **1993**, *90*, 3583−3587.
(42) Ewing, T. J.; Makino, S.; Skillman, A. G.; Kuntz, I. D. DOCK 4.0: Search Strategies for Automated Molecular Docking of Flexible Molecule Databases. *J. Comput. Aided Mol. Des.* **2001**, *15*, 411−428.
(43) Schmidt, M. W.; Baldridge, K. K.; Boatz, J. A.; Elbert, S. T.; Gordon, M. S.; Jensen, J. H.; Koseki, S.; Matsunaga, N.; Nguyen, K. A.; Su, S.; Windus, T. L. The General Atomic and Molecular Electronic Structure System. *J. Comput. Chem.* **1993**, *14*, 1347−1358.
(44) Takacs-Novak, K., Noszal, B., Hermecz, I., Kereszturi, G., Podanyi B., Szasz G. Protonation Equilibria of Quinolone Antibacterials. *J. Pharm. Sci.* **1990**, *79*, 1023−1028.
(45) Ronald, J. R.; Scheiber, R. S. In *Organic Syntheses: An Annual Publication of Satisfactory Methods for the Preparation of Organic Chemicals*; Snyder H. R., et al., Eds.; John Wiley & Sons: New York, 1948; Vol. 28, pp 38−41.

(46) Meijer, L.; Skaltsounis, A. L.; Magiatis, P.; Polychronopoulos, P.; Knockaert, M.; Leost, M.; Ryan, X. P.; Vonica, C. D.; Brivanlou, A.; Dajani, R.; Tarricone, A.; Musacchio, A.; Roe, S. M.; Pearl, L.; Greengard, P. GSK-3 Selective Inhibitors derived from Tyrian Purple indirubins. *Chem. Biol.* **2003**, *10*, 1255−1266.

(47) Wallace, A. C.; Laskowski, R. A.; Thornton, J. M. LIGPLOT: A Program To Generate Schematic Diagrams of Protein−Ligand Interactions. *Protein Eng.* **1995**, *8*, 127−134.

JM050048T